PET/MR in Oncology: Non–^{18}F-FDG Tracers for Routine Applications

Isabel Rauscher*[1–3], Matthias Eiber*[2,4], Michael Souvatzoglou[2], Markus Schwaiger[2], and Ambros J. Beer[2]

[1]*German Cancer Consortium (DKTK), Heidelberg, Germany;* [2]*Department of Nuclear Medicine, Technische Universität München, Munich, Germany;* [3]*German Cancer Research Center (DKFZ), Heidelberg, Germany; and* [4]*Department of Diagnostic and Interventional Radiology, Technische Universität München, Munich, Germany*

PET/MR is a new multimodal imaging technique that is expected to improve diagnostic performance, especially in oncologic patients in certain indications. Apart from the clinical relevance of PET with ^{18}F-FDG, various other tracers exist and are increasingly used, which allow insights into multiple physiologic and biologic processes. In this review, we discuss the current and potential future applications of hybrid PET/MR, focusing on non–^{18}F-FDG tracers. The combination of PET and MR in hybrid whole-body PET/MR systems has the potential to combine excellent morphologic, functional, and biologic information in 1 imaging session with precise image coregistration, thus paving the way for the concept of multimodal multiparametric imaging for future more widespread clinical use.

Key Words: PET/MR; non–^{18}F-FDG; oncology

J Nucl Med 2014; 55:25S–31S
DOI: 10.2967/jnumed.113.129536

PET/MR is a promising new technique, as demonstrated by several first proof-of-principle papers with ^{18}F-FDG and non–^{18}F-FDG tracers, showing good image quality and high correlation of standardized uptake values, compared with PET/CT. However, because ^{18}F-FDG PET/CT with diagnostic CT is quite powerful for most oncologic indications, the ultimate benefit of PET/MR over PET/CT has yet to be demonstrated. For some indications in which non–^{18}F-FDG tracers are used for routine diagnostics, this benefit might be easier to define: for example, PET/MR with ^{68}Ga-labeled somatostatin analogs for neuroendocrine tumors (NETs) or PET/MR with choline-labeled isotopes for prostate cancer. For both indications, the information MR can provide (e.g., soft-tissue contrast, perfusion, and diffusion-weighted imaging) might be especially beneficial, compared with CT.

In this review, we cover the available first experiences with oncologic PET/MR in clinical routine using non–^{18}F-FDG tracers and then outline the potential value of non–^{18}F-FDG tracers for which data on PET/MR are still rare (e.g., prostate-specific membrane antigen ligands). Especially with these agents, multimodal multiparametric imaging might offer additional value. In parts of this article, we also refer to our own experiences with PET/MR that have not yet been published and thus should not be misinterpreted as evidence-based knowledge but might be informative for current and future users of PET/MR, because the technique still is quite new and experience limited.

Received Mar. 21, 2014; revision accepted Apr. 24, 2014.
For correspondence or reprints contact: Ambros J. Beer, Department of Nuclear Medicine, Technische Universität München, Ismaninger Strasse 22, 81675 Munich, Germany.
E-mail: ambros.beer@uniklinik-ulm.de
*Contributed equally to this work.
Published online May 12, 2014.

ENDOCRINE

NETs are a heterogeneous group of neoplasms originating from the neural crest. The incidence of NETs has been increasing over the past 30 y as documented by Yao et al. who analyzed the Surveillance, Epidemiology and End Results database in the United States. Overall, the incidence rate in the United States increased from 10.9 per million to 52.4 per million from 1973 to 2004. From these combined registry data, the incidence is now recognized as 38 per million persons per year referenced to 2004 in the United States. The main localization of NETs is in the gastroenteropancreatic tract, followed by the lung and, rarely, the ovary and thymus (*1*,*2*). NETs are often difficult to localize using conventional morphologic imaging techniques, because they can occur throughout the body and might still be relatively small, although the patient already presents with first symptoms. A feature common to almost all NETs is the expression of somatostatin receptors, providing a unique target for their diagnosis and treatment. Therefore, radiolabeled somatostatin analogs have been used for the detection of NETs with a high sensitivity and specificity for many years as somatostatin receptor scintigraphy (SRS), often in combination with conventional morphologic imaging methods such as CT. However, SRS has several limitations: the spatial resolution of scintigraphy including SPECT is limited, and moreover the examination is relatively time-consuming, requiring imaging sessions on 2 consecutive days (*3*). A substantial progress was the introduction of SPECT/CT, which facilitates anatomic colocalization of foci of tracer uptake and differential diagnosis, for example, differentiation from unspecific uptake in the intestine (*4*). However, even SPECT/CT suffers from the inherent limitations of scintigraphic techniques; thus, the introduction of somatostatin-based radiotracers for PET imaging was a major step forward (*4*). Several studies have indicated that somatostatin receptor ligand (SRL) PET/CT has a significantly higher performance than SRS and CT in the detection and localization of the primary tumor and staging of NETs (*5*–*8*). Despite the higher performance of PET than SRS, the detection of small (<5 mm) liver lesions is still impaired because of the substantial physiologic tracer uptake of the liver. Although here dual-phase diagnostic CT can help, the detection rate usually is still lower than that of state-of-the-art MR imaging of the liver including dynamic contrast-enhanced imaging and

diffusion-weighted imaging (DWI) (*9,10*). Thus, combining PET and MR imaging should be of synergistic value in this setting. A study comparing PET/CT and whole-body MR imaging showed comparable overall lesion-based detection rates for metastatic involvement in NETs but significantly different organ-based detection rates, with superiority of PET/CT for lymph node and pulmonary lesions and of whole-body MR imaging for liver and bone metastases (*11*). This result also suggests that PET/MR could be of synergistic value, however, with the exception of small lung lesions. In line with these expectations, first studies evaluating the feasibility of ^{68}Ga-DOTATOC PET/MR imaging in comparison with PET/CT in patients with NETs showed promising results, although these first studies focused more on methodologic aspects (*12,13*). In the study of Gärtner et al. (*12*), the detectability and the standardized uptake value of focal PET lesions in PET/MR was equivalent to PET/CT on a patient basis and organ system basis. Artifacts in the form of reduced activity adjacent to regions with high physiologic activity, such as the urinary bladder, were observed predominantly on the PET/MR acquisition, which is probably related to problems with scatter correction in conjunction with attenuation maps generated from the Dixon sequence. These artifacts might have a negative impact in the detection of focal lesions in these areas; however, these technical problems inherent to all novel techniques are currently being addressed by the vendors and various research groups.

Fully diagnostic PET/MR acquisition protocols for patients with NETs have not been evaluated yet. Initial studies using retrospective image fusion showed that gadoxetate-enhanced ^{68}Ga-DOTATOC PET/MR imaging and ^{68}Ga-DOTATOC PET/DWI were equally useful for the assessment of abdominal NETs whereas another study demonstrated special advantages of ^{68}Ga-DOTATOC PET/MR imaging in patients with NET in the characterization of abdominal or liver lesions due to DWI (*14,15*). Nevertheless, the additional value of DWI in the detection and characterization of NETs is still under debate. Yet certain weaknesses inherent to MR imaging of the chest remain, because MR imaging is limited by low proton densities of the lung parenchyma and fast transverse magnetization decay.

Stolzmann et al. detected fewer lung lesions using a 3-dimensional (3D) Dixon-based, dual-echo gradient pulse sequence than low-dose CT in a trimodality PET/CT-MR set-up; however, no statistically significant differences were observed on a patient-based evaluation (*16*). In our own experience (*17*), adding a diagnostic fat-saturated contrast-enhanced gradient echo (GRE) sequence in inspiration significantly improved the detection rate of lung lesions, compared with the use of the T1-weighted GRE Dixon for attenuation correction. However, the detection rate of small lung lesions is still inferior, compared with PET/CT with diagnostic CT of the chest. Therefore, we recommend an additional chest CT in low dose if lung metastases are clinically relevant and the patient does not present with previous examinations. Our basic protocol for SRL PET/MR is shown in Supplemental Table 1 (supplemental materials are available at http://jnm.snmjournals.org).

In Figure 1, we show representative ^{68}Ga-DOTATOC PET/CT and PET/MR images in a patient with a biopsy-proven NET of the pancreas and a liver metastasis, which can be identified easily with the PET part of PET/MR and combined PET/MR with the intense ^{68}Ga-DOTATOC uptake (Figs. 1A and 1B). Although the liver metastasis can already be diagnosed in the arterial phase of the CT (Fig. 1C), the precise dimension of the primary tumor in the pancreatic head remains unclear. Only additional PET/MR depicted the exact borders of the pancreatic tumor by lower contrast enhancement (Fig. 1D) and diffusion restriction (Fig. 1E). Thus, the tumor in the pancreatic head can be differentiated clearly from unspecific tracer uptake in the uncinate process, which is a common pitfall in SRL PET.

In summary, SRL PET/MR is one of the promising clinical applications, especially when radiation exposure from CT might be an issue, for example, in younger patients or for repeated follow-up examinations, although the data in the literature are still scarce. We find SRL PET/MR in our clinical experience most useful when metastatic spread is limited and when the liver and pancreas are the focus of interest. However, in the beginning for primary staging, a diagnostic CT of the chest is advisable additionally to rule out small lung lesions. For follow-up in most instances, either PET/MR with an axial fat-saturated GRE sequence in inspiration should detect most clinically relevant lung metastases or a low-dose CT in inspiration without contrast can quickly be added to PET/MR. This strategy, however, should be evaluated in future prospective studies. In contrast to PET/MR, in our experience SRL PET/CT with diagnostic dual-phase CT is more useful for indications in which the focus is on mesenteric/peritoneal lesions or when there is widespread metastatic disease. Here, the potential advantages of MR imaging such as a detailed analysis of the liver are most likely not clinically relevant anymore.

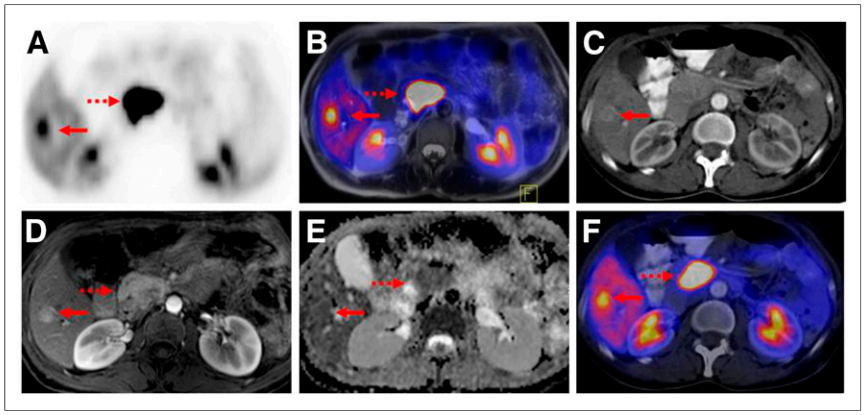

FIGURE 1. Simultaneously acquired ^{68}Ga-DOTATOC PET/CT and PET/MR images in 41-y-old patient with biopsy-proven NET of pancreas (dotted arrow) and liver metastasis in lateral fifth segment of liver (solid arrow) are shown. PET part of PET/MR (A), PET/MR (B), and PET/CT (F) images show intense focal ^{68}Ga-DOTATOC uptake in pancreatic head and location of liver metastasis. In corresponding CT scan, liver metastasis can be clearly identified, with its peripheral arterial contrast enhancement (C), whereas identification of primary tumor in pancreatic head is difficult. In corresponding MR images, there is intense arterial hyperperfusion of liver metastasis and pancreatic head in dynamic GRE sequence (D) and low apparent diffusion coefficient values both in pancreatic head and in location of liver metastasis, indicating diffusion restriction (E).

PROSTATE

Globally, prostate cancer is the cancer with the highest prevalence in men, leading to substantial morbidity and mortality (*18*). After definitive therapy with surgery or radiation, up to 50% of the patients show a biochemical recurrence (*19–21*). Currently, different guidelines name multiparametric

MR imaging as the modality of choice for detection of primary prostate cancer, especially in the setting of primary negative biopsies (*22*). In addition, depending on the availability of the different tracers used for prostate cancer imaging and the local conventions, PET/CT is used for restaging of recurrent disease and individually also for staging of primary disease (*23*).

The development of PET/MR holds great promises to improve the diagnostic accuracy of prostate cancer. MR imaging shows excellent soft-tissue contrast and a high spatial resolution, can clearly discriminate the peripheral from the central and transition zone, and can provide functional information for DWI and dynamic contrast-enhancement series. The PET part of PET/MR can provide molecular information depending on the specific tracer used (e.g., 18-fluordihydrotestosterone, ^{11}C-acetate, ^{11}C-methionine, and ^{11}C-labeled or ^{18}F-labeled choline derivatives). ^{18}F-FDG PET has some utility in castrate-resistant metastatic prostate cancer but not in the staging of primary prostate cancer or in the detection of early recurrence (*24*). Furthermore, the renal excretion of radiotracer and accumulation in the urinary bladder can impair the visualization in the pelvis. Several new tracers for targeting prostate-specific membrane antigen (PSMA) are now available (e.g., ^{68}Ga-PSMA) for PET, offering the possibility of even more tumor-specific imaging.

^{11}C-choline is a radiopharmaceutical potentially useful for prostate imaging because it is incorporated in the cell membranes as phosphatidylcholine. In contrast to ^{18}F-marked radiotracers, several studies verified that the urinary activity of ^{11}C-choline is negligible, allowing a much better delineation of the prostate fossa. One major disadvantage of ^{11}C-labeled radiotracers is the comparatively short half-life of only 20 min, limiting the use of this tracer to centers having an on-site cyclotron.

Compared with ^{18}F-FDG, ^{11}C-choline shows a considerably higher uptake in both primary prostate cancer and metastatic sites. However, ^{11}C-choline PET/CT has shown limitations for the detection of primary prostate cancer (*25–27*) because of the insufficient differentiation between benign changes such as prostatitis, high-grade intraepithelial neoplasia, or prostatic hyperplasia. In addition, especially small and rindlike tumors can often not be visualized (*25,28*). Despite promising initial results, several recent publications state a limited diagnostic accuracy, mainly because of a low sensitivity of ^{11}C-choline in detecting lymph node metastases in primary prostate cancer (*29,30*).

In the restaging of prostate cancer recurrence, ^{11}C-choline PET/CT is regarded as a valuable tool for the detection of local regional disease as well as nodal and bone metastases. However, the detection rate of ^{11}C-choline PET/CT depends on the serum prostate-specific antigen (PSA) value in patients with biochemical recurrence of prostate cancer after primary therapy, with the detection rate consistently improving from 36% for a PSA value of less than 1 ng/mL to 73% for a PSA value of 3 ng/mL or more (*31*). In clinical practice, the value of ^{11}C-choline is as PET radiotracer consists mainly in patients with biochemical recurrence presenting with a PSA level more than 1 ng/mL.

For PET/MR, a recent study by Souvatzoglou et al. (*32*) showed that the performance of integrated whole-body ^{11}C-choline PET/MR was comparable to that of PET/CT in detecting lesions with increased ^{11}C-choline uptake. Anatomic allocation of lesions was better with simultaneous PET/MR than with PET/CT, especially in the prostate and in the bone. From a technical point of view, the maximum and mean lesional standardized uptake values showed highly significant correlations between PET/CT and PET/MR ($\rho = 0.87$ and 0.86; $P < 0.001$), going along with a nearly identical number of detected lesions by visual analysis.

Promising results for the use of ^{11}C-choline PET/MR for restaging prostate cancer can be derived from a recent study stating that multiparametric MR is superior to ^{11}C-choline PET/CT in the detection of local recurrence (*33*). These findings agree with different reports in the literature expressing an additional value for the application of functional MR techniques in local recurrent disease.

Regarding lymph node metastases, preliminary results indicate a similar detection rate between ^{11}C-choline PET/MR and PET/CT (*34*). In theory, PET/MR could profit from the use of DWI as an additional tool for characterization of lymph nodes as indicated in preliminary studies (*35*). However, the additional benefit to ^{11}C-choline has yet to be evaluated, and recent publications do not show an additional value of DWI to ^{11}C-choline PET in the detection of lymph node metastases in primary prostate cancer (*29,36*).

Despite in principle high sensitivity of ^{11}C-choline PET for bone metastases, in some patients osteoblastic lesions with high density can exhibit low radiolabeled choline uptake (*37,38*). A study comparing ^{11}C-choline PET/CT and whole-body MR imaging concerning bone metastases concluded that the combination of both methods improved diagnostic accuracy (*39*).

For primary prostate cancer and its differentiation from benign changes, it is difficult to predict whether combining multiparametric MR imaging and ^{11}C-choline PET may potentially overcome the limitation of ^{11}C-choline PET/CT. The potential advantages of PET/MR are the added use of DWI, dynamic contrast-enhanced MR imaging, and MR spectroscopy imaging whereas several studies show that the combination of conventional (T2-weighted [T2w]) with functional MR imaging techniques is more reliable for differentiating benign and malignant prostate tissues than any other diagnostic procedure (*40,41*). Here, one interesting clinical application is the use of ^{11}C-choline PET/MR for biopsy targeting, especially in cases with prior negative biopsy and still high suggestion of prostate cancer (*42*). In this setting, PET/MR is of special relevance, because of the better localization of foci of choline uptake to different regions of the prostate and a better differential diagnosis of additional suspected tumors and more likely unspecific tracer uptake. In our experience, the added information of high-resolution 3D T2w imaging, DWI, and dynamic contrast-enhanced MR imaging is most useful.

The main indication for ^{11}C-choline PET/MR in prostate cancer will be the evaluation of patients with a rising PSA serum level because the detection rate of ^{11}C-choline PET/CT for the recurrence of prostate cancer is known to be limited in patients with low PSA values and a long doubling time (*31,43*). Moreover, PET/MR is of special value, when we expect more likely a local recurrence. Thus, in our practice, especially, patients presenting with a slowly increasing PSA value after radical prostatectomy are preferably scheduled for a PET/MR examination. Here, multiparametric MR of the pelvis (T2w, DWI, dynamic contrast-enhanced sequences) included in our protocol can potentially add useful diagnostic information. Because of the sometimes limited visualization of lymph nodes in MR, PET/CT might be sufficient or even superior when rather distant metastases/lymph node metastases are expected. Supplemental Figure 1 shows representative ^{11}C-choline PET/CT and PET/MR images of a patient with recurrent prostate cancer.

Recent studies have reported about a novel and highly promising method involving PET imaging with radiolabeled PSMA ligands

(*44–46*). PSMA is a cell surface protein with high expression in prostate cancer cells. In a preliminary study, the biodistribution of the novel ^{68}Ga-PSMA tracer and its ability to detect prostate cancer lesions was already analyzed using PET/CT. Lesions suggestive of prostate cancer presented with excellent contrast as early as 1 h after injection, with high detection rates even at low PSA levels. A recently published study comparing PET imaging with a ^{68}Ga-labeled PSMA ligand and ^{18}F-choline-based PET/CT for the diagnosis of recurrent prostate cancer revealed that ^{68}Ga-PSMA PET/CT can detect lesions characteristic for prostate cancer with improved contrast when compared with standard ^{18}F-fluoromethylcholine PET/CT, especially at low PSA levels (*47*).

Since ^{11}C-choline is known to be not very specific, also showing uptake in benign prostate conditions such as hyperplasia, ^{68}Ga-labeled PSMA ligand might be superior to choline tracers as it obtains a high and specific contrast. ^{68}Ga-labeled PSMA ligands are renally excreted and are highly accumulated in the bladder, thus small local recurrences might be missed by PET/CT. In these difficult cases, PET/MR offers the potential of additional function information from multiparametric MR. A recent study comparing PET/CT and PET/MR imaging hybrid systems using a ^{68}Ga-labeled PSMA ligand for the diagnosis of recurrent prostate cancer showed that prostate cancer was detected more easily and accurately with ^{68}Ga-PSMA PET/MR imaging than with PET/CT, also clarifying unclear findings on PET/CT (*48*). However, in the PET part of PET/MR imaging, artifacts from insufficient scatter correction can lead to reduced signal at the level of the kidneys and around the urinary bladder, leading to reduced standardized uptake values in some lesions. The administration of furosemide at the time of tracer injection to enhance diuresis substantially reduces these artifacts in our experience.

Our standard protocol for ^{68}Ga-PSMA PET/MR is identical to the protocol presenting for ^{11}C-choline PET/MR with the exception of a longer (+1 min) emission time for PET as seen in Supplemental Table 1. In our experience, a longer PET exam is needed for PSMA because of the relatively low radioactivity of the injected tracer. Similar to ^{11}C-choline, we prefer scheduling patients with a high likelihood of local recurrence especially with low PSA values (<1 ng/mL) on PET/MR, compared with PET/CT. In addition, examinations requesting for primary staging and biopsy targeting are preferably performed on PET/MR whereas for accurate local staging an isotropic (0.6 mm) 3D T2w sequence of the prostate is performed, providing excellent anatomic delineation.

In Figure 2, ^{68}Ga-PSMA PET/MR images of a 63-y-old patient at a PSA level of 6.35 ng/mL are shown. PET of PET/MR shows an intense focal ^{68}Ga-PSMA uptake in the right seminal vesicle, with corresponding T2 hypointensity in the MR image (Fig. 2).

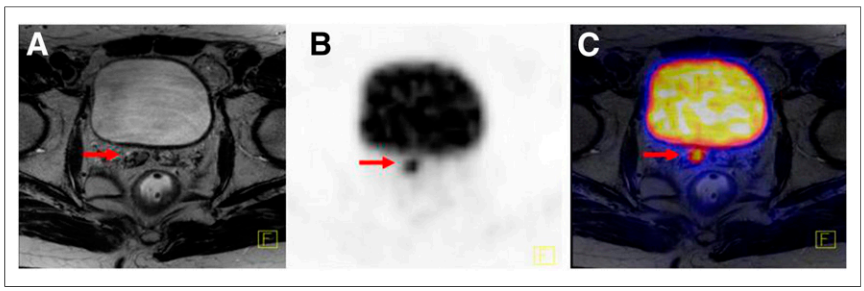

FIGURE 2. Axial ^{68}Ga-PSMA PET/MR images of 63-y-old patient with recurrent prostate cancer with hypointense signal alterations in T2w images (A, arrow) and intense focal ^{68}Ga-PSMA uptake in right seminal vesicle of PET part of PET/MR (B, arrow) and in fused PET with T2w images (C arrow).

BONE METASTASES

The skeletal system is one of the most common locations for metastasis from primary tumors such as breast, lung, thyroid gland, and prostate cancer. Therefore, it is highly important to accurately assess manifestations of malignant diseases within the bone marrow. Compared with other imaging modalities such as radiography, CT, or bone scintigraphy, MR imaging is the most sensitive technique for the detection of pathologies restricted to the bone marrow by demonstrating signal alterations due to changes in its fat, water, and hematopoietic cell components even if trabecular bone is not destroyed (*49,50*). Additionally, MR imaging allows visualization of tumor infiltration, for example, into the spinal canal or paravertebral soft tissues. Thus, potential advantages of PET/MR, compared with PET/CT, are expected in this respect.

From a metabolic point of view, the positron emitter ^{18}F-fluoride has a long history as a tracer for bone imaging. ^{18}F-fluoride is a tracer that mainly depicts blood flow and osteoblastic activity. After intravenous administration, ^{18}F-fluoride is distributed through the bone capillaries and becomes bound by chemisorption at the surface of bone crystals where they form the mineral fluoroapatite within the bone, especially at sites of bone remodelling (e.g., induced by osteoblastic activity in bone metastases). ^{18}F-fluoride allows imaging shortly (~30 min) after intravenous administration, in contrast to the significantly longer uptake times of ^{99m}Tc-labeled bisphosphonates (*51,52*). After its introduction by Blau et al. in 1962, ^{18}F-fluoride became the standard agent for bone scanning until the development of ^{99m}Tc-labeled bisphosphonates in the 1970s (*53,54*). ^{18}F-fluoride reemerged with the introduction of PET and PET/CT, which allows assessment of bone diseases with a higher spatial resolution than planar imaging or SPECT. Because of the broad availability, the simple synthesis of ^{18}F-fluoride, and the relative shortage of ^{99m}Tc, PET imaging of bone metastases with ^{18}F-fluoride might gain more importance in the future.

^{18}F-fluoride PET shows an elevated sensitivity for both osteoblastic and lytic lesions (*51,55*), compared with bone scintigraphy (*56–58*). Although the ^{18}F-fluoride uptake mechanism corresponds to osteoblastic activity, it is also highly sensitive for the detection of lytic and early marrow-based metastases. The reactive osteoblastic activity, which accompanies lytic lesions and malignant marrow deposits, is reflected by increased uptake of ^{18}F-fluoride in the periphery of the lesions, even when minimal (*56,59*).

However, several studies have analyzed ^{18}F-fluoride uptake in patients with malignant and benign diseases and showed that it is not possible to differentiate benign from malignant lesions based on the intensity of ^{18}F-fluoride uptake (*60*). Lesions detected on ^{18}F-fluoride PET, therefore, often require correlation with morphologic CT or MR imaging. Thus, studies revealed a statistically significant improvement in the specificity of ^{18}F-fluoride PET/CT, compared with ^{18}F-fluoride PET alone (*55,58*).

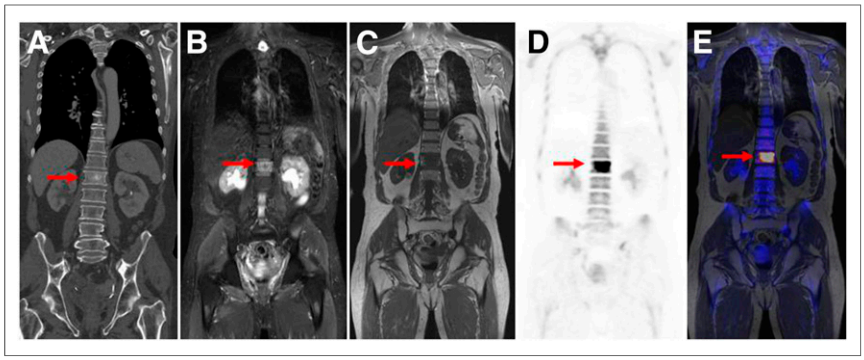

FIGURE 3. CT and ^{18}F-fluoride PET/MR images of 64-y-old patient with prostate cancer and bone metastases with coronal CT images (A, arrow), coronal T2 short τ inversion recovery (B, arrow), and T1 TSE (C, arrow). PET of PET/MR shows intense focal ^{18}F-fluoride uptake (D, arrow) whereas fused ^{18}F-fluoride PET image with simultaneously acquired T1 TSE image (E) demonstrates concordance of metabolic and anatomic imaging.

Thus, combined PET/MR imaging can offer an important tool for the early detection of bone metastasis, combining the superb imaging lesion-to-background ratio of ^{18}F-fluoride PET and the high accuracy of unenhanced T1-weighted images in demonstrating the bone marrow infiltration of metastatic disease. Hereby, because of the excellent soft-tissue contrast and high resolution of MR imaging in comparison to PET/CT the precise dimension of bone marrow infiltration could be better described before osseous destruction becomes apparent in CT. In a recent study, the performance of ^{18}F-FDG PET/MR in malignant bone lesions, compared with PET/CT, was stated as technically and clinically robust despite differences in attenuation correction (*61*). In this study, PET/MR, including diagnostic T1-weighted turbo spin echo (TSE) sequences, was superior to PET/CT for anatomic delineation and allocation of bone lesions. However, thus far no study has been published evaluating the performance of ^{18}F-fluoride PET/MR in benign or malignant disorders. Nevertheless, attenuation correction in PET/MR is still an unsolved problem. CT data simulating treating bone as soft tissue, as it is currently done in MR maps for PET attenuation correction, leads to a substantial underestimation of tracer uptake in bone lesions and depends on lesion composition, the largest error being seen in sclerotic lesions. Therefore, depiction of cortical bone and other calcified areas in MR attenuation maps is necessary for accurate quantification of tracer uptake values in PET/MR imaging (*62*).

A potential additional advantage of ^{18}F-fluoride consists in the evaluation of therapy response such as chemotherapy or radiation therapy in bone metastases. When solely MR imaging is used, it has to be considered that necrotic bone metastases may remain virtually unchanged in morphology or signal characteristics (*63*). Additionally, reduction in tumor size may be delayed and is therefore not a sensitive tool for therapy response. Though combined whole-body PET/MR may overcome this limitation because of the additional metabolic information of ^{18}F-fluoride. Hereby, MR imaging can also add valuable information in cases when initially ^{18}F-fluoride uptake might be increased after the start of therapy (e.g., flare phenomenon) (*64*).

In Figure 3, representative CT and ^{18}F-fluoride PET/MR images of a 64-y-old patient with a bone metastasis of a prostate cancer are shown. The initial obtained CT scan shows only a rather slight hypersclerosis in the body of the first lumbal vertebrae (Fig. 3A), which could have been easily missed. The additional obtained ^{18}F-fluoride PET/MR scan clearly demonstrates a high focal uptake of ^{18}F-flouride nearly in the whole vertebra (Figs. 3D and 3E). In addition, the subtotal bone marrow infiltration in the unenhanced T1-weighted sequence can be regarded as diagnostic for a bone marrow metastasis (Fig. 3C). T2w STIR shows bone marrow edema in the corresponding region, thus serving as a screening tool in most cases for bone metastases (Fig. 3B). However, the lesion-to-background contrast is much higher in PET.

For detection of bone metastases using ^{18}F-fluoride PET/MR, we prefer the use of coronal unenhanced T1 TSE and coronal turbo short τ inversion recovery T2 sequences covering the whole body from the head to toes. This protocol is adapted from whole-body MR protocols for bone screening, which have proved to be highly sensitive in discriminating benign from malignant marrow disorders (*65*). Although several studies state that DWI can offer incremental value in the detection of bone metastases (*66,67*), we do not use this sequence for routine oncologic PET/MR examinations because image acquisition with regard to whole-body coverage is time-consuming and the additional information provided by the PET part of PET/MR imaging is sufficient.

CONCLUSION

This article provides an overview of non–^{18}F-FDG PET tracers already evaluated in a PET/MR setting and their potential application in clinical routine. PET/MR is a promising new imaging tool, especially for the diagnostic work-up in patients with cancer, delivering a sensitive whole-body survey, combining molecular, functional, and anatomic data in only 1 examination. Especially because the list of radiotracers is continuously increasing, PET/MR has great potential in a more comprehensive, more accurate, and earlier diagnosis of various tumors. As discussed in this article, oncologic PET/MR using non–^{18}F-FDG tracers is potentially most valuable for NETs primarily involving the liver or pancreas and for recurrent prostate cancer. However, it has to be stressed that this statement reflects our personal opinion based on our own clinical experience. Because currently only first preliminary data based on small sample sizes are available, further prospective studies have to evaluate the most appropriate clinical applications. Hereby, the potential diagnostic benefit, compared with existing diagnostic techniques, technical feasibility, practicality, and cost, have to be considered.

DISCLOSURE

No potential conflict of interest relevant to this article was reported.

REFERENCES

1. Modlin IM, Lye KD, Kidd M. A 5-decade analysis of 13,715 carcinoid tumors. *Cancer.* 2003;97:934–959.
2. Oberg K, Castellano D. Current knowledge on diagnosis and staging of neuroendocrine tumors. *Cancer Metastasis Rev.* 2011;30(suppl 1):3–7.
3. Teunissen JJ, Kwekkeboom DJ, Valkema R, et al. Nuclear medicine techniques for the imaging and treatment of neuroendocrine tumours. *Endocr Relat Cancer.* 2011;18(suppl 1):S27–S51.

4. Wong KK, Waterfield RT, Marzola MC, et al. Contemporary nuclear medicine imaging of neuroendocrine tumours. *Clin Radiol.* 2012;67:1035–1050.
5. Geijer H, Breimer LH. Somatostatin receptor PET/CT in neuroendocrine tumours: update on systematic review and meta-analysis. *Eur J Nucl Med Mol Imaging.* 2013;40:1770–1780.
6. Gabriel M, Decristoforo C, Kendler D, et al. ^{68}Ga-DOTA-Tyr3-octreotide PET in neuroendocrine tumors: comparison with somatostatin receptor scintigraphy and CT. *J Nucl Med.* 2007;48:508–518.
7. Baum RP, Prasad V, Hommann M, et al. Receptor PET/CT imaging of neuroendocrine tumors. *Recent Results Cancer Res.* 2008;170:225–242.
8. Prasad V, Ambrosini V, Hommann M, et al. Detection of unknown primary neuroendocrine tumours (CUP-NET) using ^{68}Ga-DOTA-NOC receptor PET/CT. *Eur J Nucl Med Mol Imaging.* 2010;37:67–77.
9. Dromain C, de Baere T, Lumbroso J, et al. Detection of liver metastases from endocrine tumors: a prospective comparison of somatostatin receptor scintigraphy, computed tomography, and magnetic resonance imaging. *J Clin Oncol.* 2005;23:70–78.
10. Li RK, Zhao J, Rao SX, et al. Primary hepatic neuroendocrine carcinoma: MR imaging findings including preliminary observation on diffusion-weighted imaging. *Abdom Imaging.* 2013;38:1269–1276.
11. Schraml C, Schwenzer NF, Sperling O, et al. Staging of neuroendocrine tumours: comparison of [^{68}Ga]DOTATOC multiphase PET/CT and whole-body MRI. *Cancer Imaging.* 2013;13:63–72.
12. Gaertner FC, Beer AJ, Souvatzoglou M, et al. Evaluation of feasibility and image quality of ^{68}Ga-DOTATOC positron emission tomography/magnetic resonance in comparison with positron emission tomography/computed tomography in patients with neuroendocrine tumors. *Invest Radiol.* 2013;48:263–272.
13. Beiderwellen KJ, Poeppel TD, Hartung-Knemeyer V, et al. Simultaneous ^{68}Ga-DOTATOC PET/MRI in patients with gastroenteropancreatic neuroendocrine tumors: initial results. *Invest Radiol.* 2013;48:273–279.
14. Regier M, Schwarz D, Henes FO, et al. Diffusion-weighted MR-imaging for the detection of pulmonary nodules at 1.5 Tesla: intraindividual comparison with multidetector computed tomography. *J Med Imaging Radiat Oncol.* 2011;55: 266–274.
15. Mayerhoefer ME, Ba-Ssalamah A, Weber M, et al. Gadoxetate-enhanced versus diffusion-weighted MRI for fused Ga-68-DOTANOC PET/MRI in patients with neuroendocrine tumours of the upper abdomen. *Eur Radiol.* 2013;23:1978–1985.
16. Stolzmann P, Veit-Haibach P, Chuck N, et al. Detection rate, location, and size of pulmonary nodules in trimodality PET/CT-MR: comparison of low-dose CT and Dixon-based MR imaging. *Invest Radiol.* 2013;48:241–246.
17. Rauscher I, Eiber M, Fürst S, et al. PET/MR imaging in the detection and characterization of pulmonary lesions: technical and diagnostic evaluation in comparison to PET/CT. *J Nucl Med.* March 20, 2014 [Epub ahead of print].
18. Siegel R, Ward E, Brawley O, et al. Cancer statistics, 2011: the impact of eliminating socioeconomic and racial disparities on premature cancer deaths. *CA Cancer J Clin.* 2011;61:212–236.
19. Freedland SJ, Presti JC Jr, Amling CL, et al. Time trends in biochemical recurrence after radical prostatectomy: results of the SEARCH database. *Urology.* 2003;61:736–741.
20. Han M, Partin AW, Zahurak M, et al. Biochemical (prostate specific antigen) recurrence probability following radical prostatectomy for clinically localized prostate cancer. *J Urol.* 2003;169:517–523.
21. Chism DB, Hanlon AL, Horwitz EM, et al. A comparison of the single and double factor high-risk models for risk assignment of prostate cancer treated with 3D conformal radiotherapy. *Int J Radiat Oncol Biol Phys.* 2004;59:380–385.
22. Hoeks CM, Barentsz JO, Hambrock T, et al. Prostate cancer: multiparametric MR imaging for detection, localization, and staging. *Radiology.* 2011;261:46–66.
23. Farsad M, Schwarzenbock S, Krause BJ. PET/CT and choline: diagnosis and staging. *Q J Nucl Med Mol Imaging.* 2012;56:343–353.
24. Jadvar H. Molecular imaging of prostate cancer with PET. *J Nucl Med.* 2013;54: 1685–1688.
25. Souvatzoglou M, Weirich G, Schwarzenboeck S, et al. The sensitivity of [^{11}C] choline PET/CT to localize prostate cancer depends on the tumor configuration. *Clin Cancer Res.* 2011;17:3751–3759.
26. Farsad M, Schiavina R, Castellucci P, et al. Detection and localization of prostate cancer: correlation of ^{11}C-choline PET/CT with histopathologic step-section analysis. *J Nucl Med.* 2005;46:1642–1649.
27. Martorana G, Schiavina R, Corti B, et al. ^{11}C-choline positron emission tomography/computerized tomography for tumor localization of primary prostate cancer in comparison with 12-core biopsy. *J Urol.* 2006;176:954–960, discussion 60.
28. Schwarzenböck S, Souvatzoglou M, Krause BJ. Choline PET and PET/CT in primary diagnosis and staging of prostate cancer. *Theranostics.* 2012;2: 318–330.
29. Heck MM, Souvatzoglou M, Retz M, et al. Prospective comparison of computed tomography, diffusion-weighted magnetic resonance imaging and [C]choline positron emission tomography/computed tomography for preoperative lymph node staging in prostate cancer patients. *Eur J Nucl Med Mol Imaging.* 2014;41: 694–701.
30. Evangelista L, Guttilla A, Zattoni F, et al. Utility of choline positron emission tomography/computed tomography for lymph node involvement identification in intermediate- to high-risk prostate cancer: a systematic literature review and meta-analysis. *Eur Urol.* 2013;63:1040–1048.
31. Krause BJ, Souvatzoglou M, Tuncel M, et al. The detection rate of [^{11}C]choline-PET/CT depends on the serum PSA-value in patients with biochemical recurrence of prostate cancer. *Eur J Nucl Med Mol Imaging.* 2008;35:18–23.
32. Souvatzoglou M, Eiber M, Takei T, et al. Comparison of integrated whole-body [^{11}C]choline PET/MR with PET/CT in patients with prostate cancer. *Eur J Nucl Med Mol Imaging.* 2013;40:1486–1499.
33. Kitajima K, Murphy RC, Nathan MA, et al. Detection of recurrent prostate cancer after radical prostatectomy: comparison of ^{11}C-choline PET/CT with pelvic multiparametric MR imaging with endorectal coil. *J Nucl Med.* 2014;55: 223–232.
34. Eiber M, Souvatzoglou M, Maurer T, et al. Initial experience in restaging of patients with recurrent prostate cancer: comparison of ^{11}C-choline-PET/MR and ^{11}C-choline-PET/CT [abstract]. *J Nucl Med.* 2013;54(suppl 2):104P.
35. Eiber M, Beer AJ, Holzapfel K, et al. Preliminary results for characterization of pelvic lymph nodes in patients with prostate cancer by diffusion-weighted MR-imaging. *Invest Radiol.* 2010;45:15–23.
36. Budiharto T, Joniau S, Lerut E, et al. Prospective evaluation of ^{11}C-choline positron emission tomography/computed tomography and diffusion-weighted magnetic resonance imaging for the nodal staging of prostate cancer with a high risk of lymph node metastases. *Eur Urol.* 2011;60:125–130.
37. Beer AJ, Eiber M, Souvatzoglou M, et al. Radionuclide and hybrid imaging of recurrent prostate cancer. *Lancet Oncol.* 2011;12:181–191.
38. Wondergem M, van der Zant FM, van der Ploeg T, et al. A literature review of ^{18}F-fluoride PET/CT and ^{18}F-choline or ^{11}C-choline PET/CT for detection of bone metastases in patients with prostate cancer. *Nucl Med Commun.* 2013;34: 935–945.
39. Eschmann SM, Pfannenberg AC, Rieger A, et al. Comparison of ^{11}C-choline-PET/CT and whole body-MRI for staging of prostate cancer. *Nuklearmedizin.* 2007;46:161–168.
40. Seitz M, Shukla-Dave A, Bjartell A, et al. Functional magnetic resonance imaging in prostate cancer. *Eur Urol.* 2009;55:801–814.
41. Sciarra A, Barentsz J, Bjartell A, et al. Advances in magnetic resonance imaging: how they are changing the management of prostate cancer. *Eur Urol.* 2011;59: 962–977.
42. Takei T, Souvatzoglou M, Beer AJ, et al. A case of multimodality multiparametric ^{11}C-choline PET/MR for biopsy targeting in prior biopsy-negative primary prostate cancer. *Clin Nucl Med.* 2012;37:918–919.
43. Castellucci P, Fuccio C, Nanni C, et al. Influence of trigger PSA and PSA kinetics on ^{11}C-choline PET/CT detection rate in patients with biochemical relapse after radical prostatectomy. *J Nucl Med.* 2009;50:1394–1400.
44. Roethke MC, Kuru TH, Afshar-Oromieh A, et al. Hybrid positron emission tomography-magnetic resonance imaging with gallium 68 prostate-specific membrane antigen tracer: a next step for imaging of recurrent prostate cancer-preliminary results. *Eur Urol.* 2013;64:862–864.
45. Afshar-Oromieh A, Haberkorn U, Hadaschik B, et al. PET/MRI with a ^{68}Ga-PSMA ligand for the detection of prostate cancer. *Eur J Nucl Med Mol Imaging.* 2013;40:1629–1630.
46. Afshar-Oromieh A, Malcher A, Eder M, et al. PET imaging with a [^{68}Ga]gallium-labelled PSMA ligand for the diagnosis of prostate cancer: biodistribution in humans and first evaluation of tumour lesions. *Eur J Nucl Med Mol Imaging.* 2013;40:486–495.
47. Afshar-Oromieh A, Zechmann CM, Malcher A, et al. Comparison of PET imaging with a ^{68}Ga-labelled PSMA ligand and ^{18}F-choline-based PET/CT for the diagnosis of recurrent prostate cancer. *Eur J Nucl Med Mol Imaging.* 2014;41: 11–20.
48. Afshar-Oromieh A, Haberkorn U, Schlemmer HP, et al. Comparison of PET/CT and PET/MRI hybrid systems using a Ga-labelled PSMA ligand for the diagnosis of recurrent prostate cancer: initial experience. *Eur J Nucl Med Mol Imaging.* 2014;41:887–897.
49. Daldrup-Link HE, Franzius C, Link TM, et al. Whole-body MR imaging for detection of bone metastases in children and young adults: comparison with skeletal scintigraphy and FDG PET. *AJR.* 2001;177:229–236.
50. Imamura F, Kuriyama K, Seto T, et al. Detection of bone marrow metastases of small cell lung cancer with magnetic resonance imaging: early diagnosis before

destruction of osseous structure and implications for staging. *Lung Cancer.* 2000;27:189–197.
51. Groves AM, Win T, Haim SB, et al. Non-[^{18}F]FDG PET in clinical oncology. *Lancet Oncol.* 2007;8:822–830.
52. Even-Sapir E, Mishani E, Flusser G, et al. ^{18}F-fluoride positron emission tomography and positron emission tomography/computed tomography. *Semin Nucl Med.* 2007;37:462–469.
53. Blau M, Nagler W, Bender MA. Fluorine-18: a new isotope for bone scanning. *J Nucl Med.* 1962;3:332–334.
54. Brenner W, Vernon C, Muzi M, et al. Comparison of different quantitative approaches to ^{18}F-fluoride PET scans. *J Nucl Med.* 2004;45:1493–1500.
55. Even-Sapir E, Metser U, Flusser G, et al. Assessment of malignant skeletal disease: initial experience with ^{18}F-fluoride PET/CT and comparison between ^{18}F-fluoride PET and ^{18}F-fluoride PET/CT. *J Nucl Med.* 2004;45:272–278.
56. Schirrmeister H, Guhlmann A, Kotzerke J, et al. Early detection and accurate description of extent of metastatic bone disease in breast cancer with fluoride ion and positron emission tomography. *J Clin Oncol.* 1999;17:2381–2389.
57. Schirrmeister H, Glatting G, Hetzel J, et al. Prospective evaluation of the clinical value of planar bone scans, SPECT, and ^{18}F-labeled NaF PET in newly diagnosed lung cancer. *J Nucl Med.* 2001;42:1800–1804.
58. Even-Sapir E, Metser U, Mishani E, et al. The detection of bone metastases in patients with high-risk prostate cancer: ^{99m}Tc-MDP planar bone scintigraphy, single- and multi-field-of-view SPECT, ^{18}F-fluoride PET, and ^{18}F-fluoride PET/CT. *J Nucl Med.* 2006;47:287–297.
59. Even-Sapir E. Imaging of malignant bone involvement by morphologic, scintigraphic, and hybrid modalities. *J Nucl Med.* 2005;46:1356–1367.
60. Cook GJ, Fogelman I. The role of positron emission tomography in skeletal disease. *Semin Nucl Med.* 2001;31:50–61.
61. Eiber M, Takei T, Souvatzoglou M, et al. Performance of whole-body integrated ^{18}F-FDG PET/MR in comparison to PET/CT for evaluation of malignant bone lesions. *J Nucl Med.* 2014;55:191–197.
62. Samarin A, Burger C, Wollenweber SD, et al. PET/MR imaging of bone lesions: implications for PET quantification from imperfect attenuation correction. *Eur J Nucl Med Mol Imaging.* 2012;39:1154–1160.
63. Schmidt GP, Reiser MF, Baur-Melnyk A. Whole-body imaging of the musculoskeletal system: the value of MR imaging. *Skeletal Radiol.* 2007;36:1109–1119.
64. Wade AA, Scott JA, Kuter I, et al. Flare response in ^{18}F-fluoride ion PET bone scanning. *AJR.* 2006;186:1783–1786.
65. Steinborn MM, Heuck AF, Tiling R, et al. Whole-body bone marrow MRI in patients with metastatic disease to the skeletal system. *J Comput Assist Tomogr.* 1999;23:123–129.
66. Nakanishi K, Kobayashi M, Nakaguchi K, et al. Whole-body MRI for detecting metastatic bone tumor: diagnostic value of diffusion-weighted images. *Magn Reson Med Sci.* 2007;6:147–155.
67. Luboldt W, Kufer R, Blumstein N, et al. Prostate carcinoma: diffusion-weighted imaging as potential alternative to conventional MR and ^{11}C-choline PET/CT for detection of bone metastases. *Radiology.* 2008;249:1017–1025.